STED-Inspired Cationic Photoinhibition Lithography

THE JOURNAL OF PHYSICAL CHEMISTRY C
A JOURNAL OF THE AMERICAN CHEMICAL SOCIETY

pubs.acs.org/JPCC
Article

STED-Inspired Cationic Photoinhibition Lithography

Sourav Islam, Marco Sangermano, and Thomas A. Klar*

Cite This: J. Phys. Chem. C 2023, 127, 18736−18744
Read Online

ABSTRACT: Direct laser writing by two-photon lithography has been enhanced substantially during the past two decades by techniques borrowed from stimulated emission depletion (STED) microscopy. However, STED-inspired lithography was so far limited to radical polymerizations, mostly to acrylates and methacrylates. Cationic polymers did not derive benefits from this technique. Specifically, epoxide polymerization, which plays a paramount role in semiconductor clean-room technology, has not yet been reported with a second, depleting laser focus in the outer rim of the point spread function. We now found that using a thioxanthone as a sensitizer and sulfonium or iodonium salts as photoinitiators enables at least partial optical on/off switching of two-photon polymerization and, in the case of the sulfonium salt, allows for writing epoxy lines with widths shrunk by approx. two-thirds compared to lines written with two-photon polymerization alone.

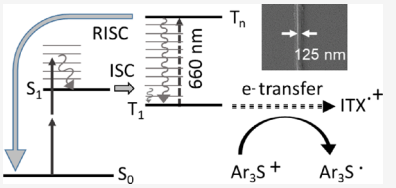

INTRODUCTION

STED-inspired lithography can be used to improve the feature widths and resolutions of multiphoton lithography (MPL), where multiple photons of a visible or near-infrared short-pulse laser are used to excite the photoinitiators.[1] Compared to standard UV-based lithography, MPL has two decisive advantages: First, it bears an intrinsic three dimensionality, and second, it uses less photon energy compared to mid- to far-UV or e-beam lithography. Unfortunately, the larger wavelength poses restrictions to the minimal feature size, being about 100 nm in the state-of-the-art acrylate-based MPL.[2,3]

In the 90s, it has been proposed[4] and experimentally shown[5] that diffraction-unlimited fluorescence microscopy is possible using stimulated emission depletion (STED) in the outer rim of the focal point spread function (PSF). Soon, it became clear that not only STED but any technique that reversibly switches off excited fluorophores by a second laser beam can in principle be used for far-field imaging beyond the diffraction limit.[6] Inspired by this success in microscopy, optical switching in the outer rim of the PSF has been applied to nanometrically control photoinitiators of radical polymerization reactions, and hence, structure sizes down to the deep-subwavelength scale could be achieved.[7−11] These and many other reports on STED-inspired photoinhibition lithography have in common that they focus on radical polymerizations, mostly of (meth)acrylates.[12] Only a few records on STED-inspired lithography beyond radical polymerization exist. For instance, individual chemical click reactions can be used, where a molecule can either be reversibly switched into a reactive isomer with one wavelength and switched back to an unreactive one with another wavelength of light,[13,14] or where individual redox reactions can be optically activated with one wavelength and prevented with another one.[15] These are individual reactions, not polymerizations; however, they can be used in a photoresist by inducing gelation.[16,17] Importantly, the relevant class of cationic (and also anionic) polymerizations eluded STED-inspired photoinhibition lithography, so far. This is all the worse as epoxy-based resins are generally less toxic and show reduced shrinkage compared to acrylates and they are the workhorse of semiconductor clean-room lithography.[18] Notably, using MPL alone to polymerize epoxides, the linewidths are typically four to five times as thick as comparable linewidths achieved with (meth)acrylates.[19,20] Consequently, the minimal feature sizes achievable by MPL are more in the range of half a micrometer in the case of epoxides, instead of 100 nm as it was achieved with acrylates.[2] From this starting point, the applicability of STED-inspired photoinhibition lithography to cationic photopolymerization would be highly welcome.

The upper line in Figure 1 shows a common strategy to photopolymerize epoxy resins. The polymerization of the monomers is optically started via an onium salt.[21,22] These photoinitiators typically show strong absorbances in the UV range below 300 nm (iodonium salts)[21] or below 350 nm (sulfonium salts)[22] but no absorption above these wavelengths. Rapidly after excitation, they initiate the polymerization via the photogenerated strong Brønsted acid through a cationic chain growth process. These facts make this classical strategy useless for our purpose for two reasons: First, we are aiming for a resist that is excitable in the very near UV (to fit a two-photon excitation by 780 nm femtosecond pulses), and second, the reaction steps after photoexcitation of the onium are "dark" in

Received: June 29, 2023
Revised: August 17, 2023
Published: September 7, 2023

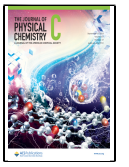

https://doi.org/10.1021/acs.jpcc.3c04394
J. Phys. Chem. C 2023, 127, 18736−18744

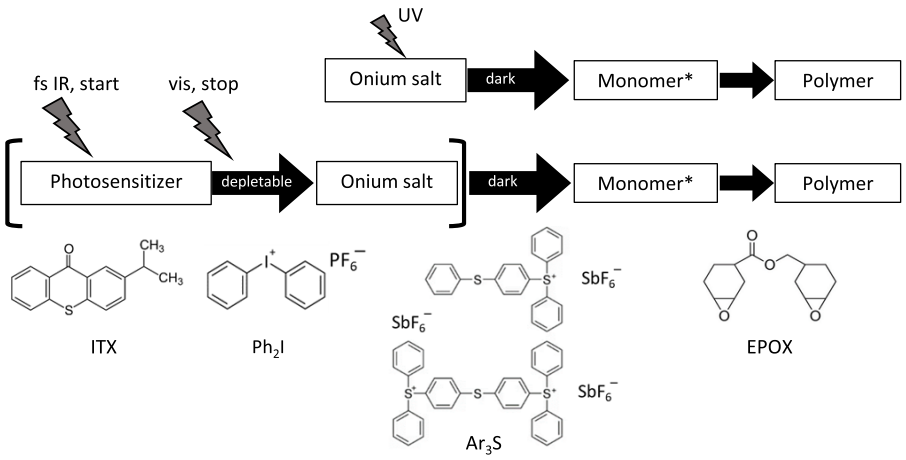

Figure 1. Upper line: usually, an onium salt is excited by UV light and activates a monomer, which then polymerizes. The process is fast and comprises optically inaccessible (dark) reactions. Middle line: a photosensitizer, excitable with near-UV or the corresponding femtosecond near-IR pulses, sensitizes the onium salt. This process is slow and can be stopped (depleted) by visible light. Lower line: structures of the used chemicals: ITX as a photosensitizer, either $Ph_2I:PF_6$ or $Ar_3S:SbF_6$ as onium salts, and EPOX as an epoxy monomer.

the sense that they cannot be manipulated optically anymore after they have been triggered by light. Hence, the reaction cannot be stopped by a second laser beam, and STED-inspired lithography will not work. The first issue has been addressed by using photosensitizers absorbing in the near-UV to blue spectral range,[23] specifically by using thioxanthones including isopropyl thioxanthone (ITX).[22,23] Boiko et al. have shown that a sensitizer/initiator doublet comprising a thioxanthone and an onium salt can also be used for MPL using a Ti:Sapphire femtosecond laser.[19] We sketch this approach in the middle line of Figure 1. Importantly, ITX is well-known to be a photoswitchable initiator, useful for STED-inspired acrylate lithography.[9] ITX proved to be optically depletable via transient-state absorption when using wavelengths from 530 to 700 nm.[24−26] In the following, we will abbreviate this process with TAD: "transient-state absorption depletion". Several other thioxanthones have been screened for STED-inspired radically polymerizing lithography; however, ITX proved to be the most effective.[27,28] Further, a large body of work, both theoretical and experimental, is available on the photophysics of thioxanthones.[29−40]

Here, we report, to the best of our knowledge for the first time, about a successful attempt to nanostructure an epoxy resist by means of STED-inspired photoinhibition lithography and show that lines written with photoinhibition show an approx. 66% smaller width compared to lines written with sheer two-photon lithography. Using published numerical values of the dynamics of ITX and similar thioxanthones' triplet states and the dynamics of photoinitiation of onium salts by ITX, we are able to give an explanation for the process of photodepletion.

MATERIALS AND METHODS

We used a homebuilt dual-beam two-photon lithography setup similar to the one described before.[11] The photoresists used for the experiments were a mixture of 3,4-epoxycyclohexylmethyl 3,4-epoxycyclohexanecarboxylate (EPOX, Sigma Aldrich) as a monomer, triarylsulfonium hexafluoroantimonate of 50 wt % in propylene carbonate ($AR_3S:SbF_6$, Sigma Aldrich, prod. no. 654027) or diphenyliodonium-hexafluorophosphate ($Ph_2I:PF_6$, Sigma Aldrich, prod. no. 548014) as onium salts, and 2-isopropylthioxanthone (ITX, Sigma Aldrich) as a photosensitizer. Several different mixtures of ITX and onium salts were investigated to find the best composition for nanofabrication (see Supporting Information, Figures S1 and S2). For both onium salts, the best results were obtained when using 4 wt % ITX and 1 wt % onium salt. Glass slides of thickness 170 ± 5 μm (Marienfeld GmbH, Germany) were precoated with (3-glycidyloxypropyl) trimethoxysilane (Sigma Aldrich) in order to achieve better adhesion between the polymer and the glass surface, and the resins were dropcast onto them. Then, a glass slide was mounted on a three-axis piezo stage (P-562.3CD, Physik Instrumente (PI), Germany) with a bidirectional positioning accuracy of 2/2/4 nm ($x/y/z$) and a 200 μm travel range in each direction. The writing speed was 2 μm/s. The ITX was excited by laser pulses of 780 nm (82 MHz repetition rate, 110 fs, FFS-tSHG, Toptica, Germany). TAD was performed via a continuous wave (CW) 660 nm laser (Opus, Laser Quantum, Germany). The power of the excitation beam was controlled by an acousto-optical modulator (MT110-A1.5-IR, AA Opto Electronic, France), while the power of the TAD beam was adjusted directly by the laser. All powers quantified in this paper were powers entering the back aperture of the objective lens (60×, NA 1.49, oil immersion, Olympus, Japan). While writing, we could observe a small point (possibly fluorescence from ITX) moving forward in the scan direction. After writing the lines, the samples were developed by rinsing with 5 to 10 drops of ethanol until the sample was visibly clean. For depletion experiments, two ordinary foci were confocalized, and the heights of the written lines were determined with an AFM (DI, CP-II, Digital Instruments, USA). In the case of STED-inspired TAD lithography, a 2π phase spiral (RPC Photonics, Rochester, NY, USA) was used to create a donut-shaped focus, placed around the 780 nm excitation focus. Linewidths were determined with a Zeiss 1540XB SEM after evaporating approx. 10 nm of gold.

EXPERIMENTAL RESULTS

In a first experiment, we wrote lines on a glass substrate using different compositions of EPOX, ITX, and onium salts and varied the two-photon excitation power. The best results for our purposes were obtained using 4 wt % ITX and 1 wt % onium salts (other compositions are shown in Supporting

https://doi.org/10.1021/acs.jpcc.3c04394
J. Phys. Chem. C 2023, 127, 18736−18744

Information, Figures S1 and S2). Excitation powers were 3.2−3.4 mW for both ITX/onium salt compositions. Without a depletion laser, the lines were typically 180 (185) nm high and 350 (500) nm wide when using $Ar_3S:SbF_6$ ($Ph_2I:PF_6$) as an onium salt, respectively. It is well-known in MPL that the heights of lines written directly on a glass substrate can be well below the axial size of the point spread function.[41] Compared to linewidths down to 100 nm achieved with high numerical aperture lens MPL lithography in acrylates,[2,3] 350 to 500 nm linewidths might sound quite large; however, we note that in the case of photochemically initiated cationic polymerization, linewidths are typically four to five times as thick as comparable linewidths achieved with (meth)acrylates.[19,20]

Starting from line heights of around 180 nm (measured with AFM), we gradually increased the depleting TAD power, confocalized with an ordinary PSF on top of the MPL excitation focus. Figure 2 shows the relative reduction in line height as a function of TAD power for both resists, ITX/$Ar_3S:SbF_6$ and ITX/$Ph_2I:PF_6$ in panels a and b, respectively. One sees a roughly exponential decrease in line height with increasing TAD power. The red lines are exponentially decaying numerical fits to the data. In both cases, the lines do not totally disappear, but residuals of 40 and 30% remain in the cases of ITX/$Ar_3S:SbF_6$ and ITX/$Ph_2I:PF_6$, respectively. Higher TAD powers than 30 or 25 mW, respectively, were not applied in order to not destroy the sample due to microexplosions caused by excessive 660 nm optical power, which occur irrespective of a simultaneous 780 nm excitation. It is quite clear that there are apparently two species of polymerizations, one that can be depleted by 660 nm light and another one that cannot and is responsible for the residual line height. We will discuss that in more detail in the Discussion section. The species, which can be depleted, showed threshold depletion powers (defined as the power where $1/e$ of the line height was reached) of P_{sat} = 1.7 ± 0.2 and 8.1 ± 1.6 mW in the case of $Ar_3S:SbF_6$ and $Ph_2I:PF_6$, respectively. These powers play a similar role in STED-inspired lithography to that played by the so-called saturation powers P_{sat} in STED microscopy, which are the depletion powers where the fluorescence has dropped down to $1/e$ of its original value without depletion. It has been shown by Hell and Westphal[42] that the minimally achievable resolution in STED microscopy as a function of the applied depletion power P_{depl} is given by

$$d = \frac{1}{\sqrt{1 + \frac{P_{depl}}{P_{sat}}}} \cdot \frac{\lambda}{2n\sin\alpha} \quad (1)$$

whereby λ is the vacuum wavelength of light, n is the refractive index of the immersion medium, and α is the half-opening angle of the objective lens. Comparing now ITX/$Ar_3S:SbF_6$ with ITX/$Ph_2I:PF_6$ as a starter system for EPOX polymerization, we can conclude that ITX/$Ar_3S:SbF_6$ bears the advantage of having the lower saturation power, while ITX/$Ph_2I:PF_6$ has the advantage of having the lower amount of undepletable background. In the discussion, we will argue that both effects are inter-related.

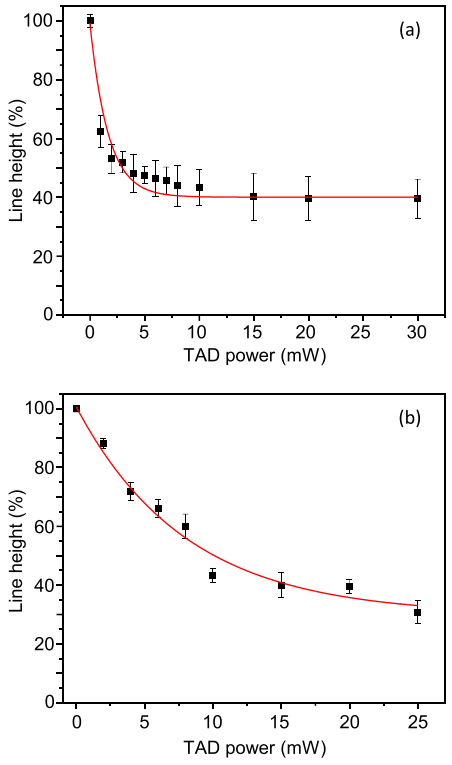

Figure 2. Suppression of polymerization: line height (measured with AFM) as a function of transient absorption depletion (TAD) power. The excitation power was 3.3 mW. Starter compositions: (a) 4 wt % ITX, 1 wt % $Ar_3S:SbF_6$ and (b) 4 wt % ITX, 1 wt % $Ph_2I:PF_6$. The red lines are fitted single-exponential decays. The residuals are 40 and 30% in the case of $Ar_3S:SbF_6$ and $Ph_2I:PF_6$, respectively. The $1/e$ exponential decay powers P_{sat} are 1.7 ± 0.2 and 8.1 ± 1.6 mW in the case of $Ar_3S:SbF_6$ and $Ph_2I:PF_6$, respectively.

The best possible depletion of the line height, ideally down to the complete vanishing of lines, as typically seen in acrylate-based STED-inspired lithography,[43] is desirable in order to achieve the narrowest feature sizes. Unfortunately, this is apparently not the case in both EPOX systems that we used in this study. Nevertheless, this does not preclude the use of these systems. In TAD lithography, a comparatively long-lived transient state is used to optically switch off the polymerization. This is somewhat related to the so-called RESOLFT (reversible saturable optical fluorescence transitions) microscopy,[6] where in diffraction-unlimited fluorescence microscopy, a long-lived state is optically manipulated. Indeed, in the first reports about RESOLFT microscopy, it was also not possible to totally switch off fluorescence with a depleting beam. Very similar to our case (c.f. Figure 2), about 40% of fluorescence could not be switched off, but still, a subdiffractional resolution was achieved.[6] Therefore, we turned to STED-inspired photoinhibition lithography.

In order to test the minimally achievable linewidths, we switched from an ordinarily shaped PSF of the 660 nm depleting beam to a donut-shaped PSF by inserting a 2π phase mask. After developing the lines, they were overcoated with 10 nm of gold and imaged in an SEM. Figure 3a shows some lines with ITX/$Ar_3S:SbF_6$ as the sensitizer/initiator system. The excitation power was 3.2 mW, and the TAD powers were as indicated. The large blobs at the beginning and ending of each line are anchoring points, written with a high excitation power of 6 mW. This fixates the lines and avoids washing them off during development. The frequently observed central hole in the middle of the anchors might be due to some ablation. When no TAD power was applied (i.e., pure MPL lithography), a linewidth of 370 nm was achieved in this example. This is a typical linewidth for MPL lithography of epoxides, where minimal linewidths are typically 3 to 5 times

https://doi.org/10.1021/acs.jpcc.3c04394
J. Phys. Chem. C 2023, 127, 18736−18744

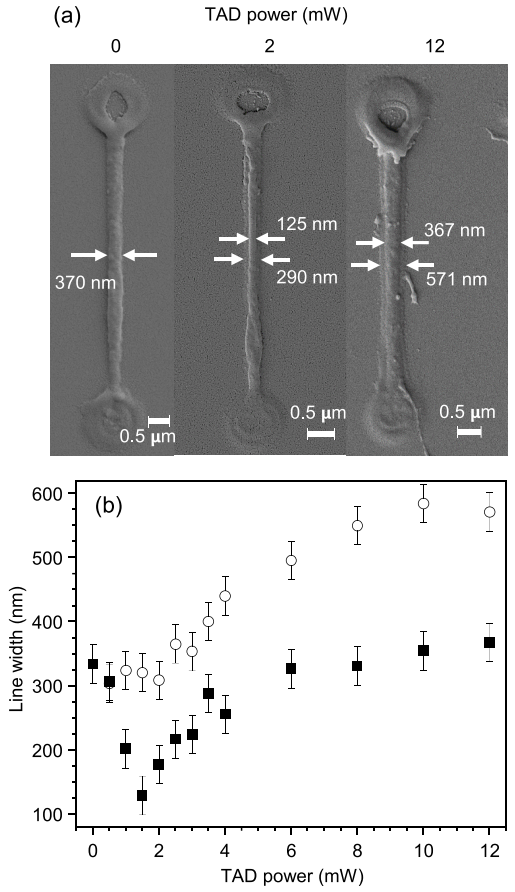

Figure 3. (a) Lines written with 3.2 mW of 780 nm excitation power and different TAD powers as indicated, using 4 wt % ITX and 1 wt % $Ar_3S:SbF_6$. The pure MPL (0 mW TAD) linewidth is 370 nm. Applying 2 mW of TAD, the central line narrows by 66% down to 125 nm, but a faint pedestal of 290 nm width is visible. In the case of 12 mW, the central line is as wide as the line without TAD, and the pedestal widens to 571 nm. (b) Widths of the central lines (filled squares) and the pedestals (open circles). Data points in (b) are averages of up to 4 independent experiments.

wider than typically achievable widths of MPL-written acrylate lines.[19,20] Applying a 2 mW TAD power, the linewidth shrank down to 125 nm in this specific case, which is a 2/3 improvement compared to the linewidth without TAD. However, on closer inspection, one recognizes a pedestal underneath the central thin line, which has a width of 290 nm. When 12 mW TAD was applied, the width of the central line was nearly as wide as the linewidth without TAD and the width of the pedestal grew up to 571 nm. We wrote lines for several other TAD powers and repeated the whole series four times. SEM images of all four runs of measurements and tables with the measured linewidths are given in the Supporting Information (Figure S4 and Tables S1 and S2). Figure 3b shows the linewidths, averaged over the four runs, as a function of TAD power. The full squares show the widths of the central lines, and the open circles show the widths of the pedestals.

When the TAD power was increased up to 1.5 mW, the width of the central lines shrank by about two-thirds down to 130 nm on average. Although this result is well above the routinely achievable linewidths of less than 50 nm in free radical-initiated, acrylate-based STED-inspired photoinhibition lithography, it is still a major achievement because this is, to the best of our knowledge, the first time that STED-inspired lithography showed a marked effect on linewidth in cationically initiated polymerization. Given the 14 years advancement of free radical-initiated STED-inspired lithography, this is a remarkable first result for STED-inspired, cationically initiated lithography.

When increasing the TAD power beyond 1.5 mW, the central lines broaden again, approaching the original linewidth from 6 mW TAD power onward. In other words, a STED-inspired line narrowing can only be observed between 0.5 and approx. 5 mW TAD power, with a minimal linewidth at 1.5 mW. In addition, the pedestal widens substantially from approx. 3 mW onward, saturating at an about 600 nm linewidth. We will suggest a reason for the origin of this pedestal in the discussion.

We also tried to write lines with the iodonium salt as a photoinitiator. Unfortunately, the results were not well-repeatable from run to run; specifically, the lines did not stick to the substrate and contained bulges and blobs. Some

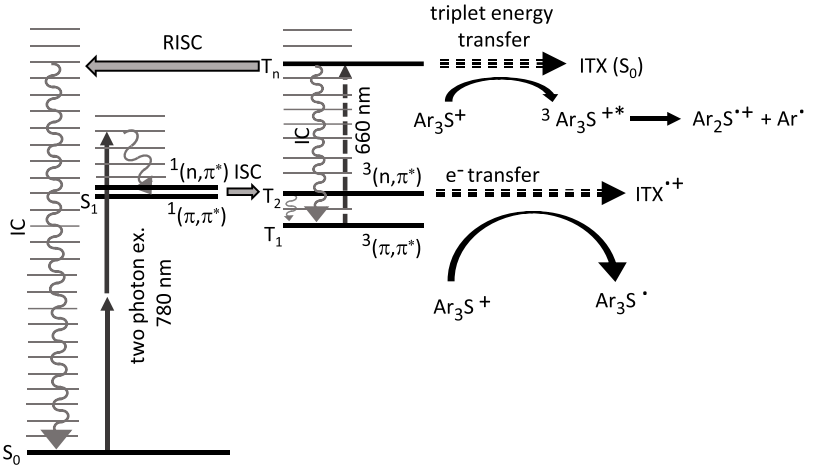

Figure 4. Jablonski diagram of ITX. After 780 nm two-photon excitation, ITX undergoes intersystem crossing (ISC) to the triplet system, from where it can excite an onium, e.g., Ar_3S^+, via electron transfer. If an additional 660 nm light is provided, ITX is further excited to T_n, from where it can either fall back to T_1 via internal conversion (IC) or undergo reverse intersystem crossing (RISC) followed by fast IC down to S_0, or it can transfer its energy to the onium. Further details are described in the text.

https://doi.org/10.1021/acs.jpcc.3c04394
J. Phys. Chem. C 2023, 127, 18736−18744

results are shown in Supporting Information, Figure S5. In the case of some rare, successfully written lines, we found a 0 mW TAD linewidth (pure MPL) of 400 to 600 nm and also observed about 2/3 shrinkage down to 220 nm when about 6 mW of TAD was applied. Beyond that TAD power, the linewidths increased again. Interestingly, the minimal linewidths achieved with $Ar_3S:SbF_6$ and $Ph_2I:PF_6$ were 1.5 and 6 mW, respectively, both powers being close to the saturation intensities P_{sat} of 1.7 and 8.1 mW obtained in the depletion experiments (Figure 2). Because of the 4.5 times higher TAD power for minimal linewidths and the overall poor performance of line stability in the case of $ITX/Ph_2I:PF_6$, we conclude that $ITX/Ar_3S:SbF_6$ is the far better photoinitiator system for STED-inspired photoinhibition lithography of EPOX.

THEORETICAL ESTIMATIONS

We herewith put our results into context with the well-established framework of ITX-sensitized initiation of cationic polymerization. The energy levels of thioxanthones have been studied in great detail before[32−36] and are summarized in Figure 4, the left part of which represents a Jabłonski diagram showing singlet and triplet levels relevant for our discussion. After two-photon excitation,[19] the ITX will temporarily be excited into a higher vibrational level of $^1(\pi,\pi^*)$, from where it quickly transfers via intersystem crossing (ISC) to $^3(n,\pi^*)$ followed by internal conversion (IC) down to $^3(\pi,\pi^*)$.[34] Alternatively, it first undergoes IC within the singlet system to $^1(n,\pi^*)$ followed by ISC to a higher vibrational level of $^3(\pi,\pi^*)$ followed by IC within the $^3(\pi,\pi^*)$.[36] Both pathways obey El-Sayed's rule,[44] which means that ISC is very effective and the ITX ends up in the triplet system after some picoseconds. It depends on the polarity of the monomer which of the two routes prevails.[34,36] As both of them equally end up in the $^3(\pi,\pi^*)$ state, it is futile and beyond the scope of this paper to discuss this in detail.

Once in the $T_1 = {}^3(\pi,\pi^*)$ state, the initiation of a cationic polymerization proceeds via a thermal repopulation of the $T_2 = {}^3(n,\pi^*)$ state followed by a rapid transfer of an electron from the sensitizing ITX toward the aryl-onium cation.[45,46] This process is shown in the lower right part of Figure 4 for the case of Ar_3S^+, but the sensitization of Ph_2I^+ via electron transfer works analogously. Although ITX is commonly called the "sensitizer", this is actually misleading because it is predominantly the resulting $ITX^{\cdot+}$ radical cation, which itself induces cationic polymerization. As the ITX needs to be thermally activated within the triplet system prior to electron transfer, the overall process is rather slow.[30,45] This gives time for the second, deactivating continuous wave (CW) laser beam of 660 nm wavelength to excite the ITX from $T_1 = {}^3(\pi,\pi^*)$ into a higher triplet level T_n via an optically allowed transient-state absorption.[45] From the T_n level, the molecule has three options to proceed: The first and most effective pathway is IC within the triplet system back down to the T_1. If we assume that IC within the singlet and within the triplet systems is of similar probability, the rate of intratriplet IC is approximately $\gamma_{TIC} = (0.4\ ps)^{-1}$.[36] The second possibility is a reverse intersystem crossing (RISC in Figure 4) followed by quick IC within the singlet system. This will bring the ITX back to the ground state and will lead to an effective transient (here: triplet)-state absorption depletion (TAD) process, which is also the core process for subdiffractional STED-inspired lithography of acrylates using ITX as a two-photon radical starter.[24−26,39,40] In the following, we assume that the rates of RISC and ISC are similar. The published timescales for ISC actually vary between 4 and 10 ps.[34,36,40] For the further discussion, we take the average and assume $\gamma_{RISC} = (7\ ps)^{-1}$, keeping in mind that this is probably the least well-known parameter in the following considerations. Nevertheless, it is for sure an order of magnitude less effective than intratriplet IC.

Even slower is a third possibility: An ITX molecule in the T_n state has sufficient energy to excite the onium via triplet energy transfer.[23,30] In this sense, ITX acts as a "true" sensitizer of the Ar_3S^+ (or the Ph_2I^+). During this process, the ITX turns from the T_n down to the S_0, and simultaneously, the Ar_3S^+ is excited to its triplet state, from where it decays into an $Ar^{\cdot}$ cation and an $Ar_2S^{\cdot+}$ radical cation, which initiates polymerization. As the ITX turns from a triplet to a singlet and the Ar_3S^+ from a singlet to a triplet, this energy transfer is spin-conserving and hence allowed. However, we assume that the rate of this third process is on a typical scale of energy transfers, which means $\gamma_{ET} = (500\ ps)^{-1}$, two orders of magnitude lower than RISC and three orders of magnitude lower than intratriplet IC.

For the time being, we will neglect the slow process of energy transfer and concentrate on the decay of the T_n on the branching ratio between RISC and intratriplet IC. In order to render TAD effective, RISC needs to outperform the thermal activation from $^3(\pi,\pi^*)$ to $^3(n,\pi^*)$ followed by an electron transfer (c.f. Figure 4). This initiation process can indeed be depleted by TAD, if the molecule is continuously being excited from the T_1 to the T_n followed by intratriplet IC back down to T_1, thereby effectively cycling the molecule between the T_1 and the T_n. Each time that the molecule is in T_n, there is a finite probability for RISC to escape this cycle and therefore to escape the triplet system. The quantum efficiency to escape per one cycle is $\eta_{esc} = \gamma_{RISC}/(\gamma_{RISC} + \gamma_{TIC}) = 5.4\%$.

In STED microscopy, a decisive parameter is the so-called saturation power P_{sat} of the STED beam, which is defined as the power where the remaining (not depleted) fluorescence has dropped down to $1/e$ of its original value.[42] Transferring this terminology to STED-inspired lithography, P_{sat} would be the power where the photoinitiation via electron transfer is depleted via TAD down to $1/e$ of its original value. In order to calculate that, we first need to know the quantum efficiency of electron transfer without TAD. If an ITX is in its $T_1 = {}^3(\pi,\pi^*)$ state, it can undergo several reactions: First, it might decay back down to S_0. This rate has been found to be $\gamma_0 = 0.1\ \mu s^{-1}$.[45] Next, it might be quenched by electron transfer to an EPOX monomer. This leads to a reduction of an EPOX monomer; however, such a reduced EPOX cannot start a polymerization reaction. Hence, this is a loss process.[45] Given a concentration of the EPOX monomer (which is the monomer and the solvent at the same time) as [EPOX] = 4.41 M and taking the rate of quenching by the monomer as $k_{EPOX} = 6.0\ M^{-1}\ \mu s^{-1}$,[45] we end up with a rate of quenching by the monomers of $\gamma_{EPOX} = k_{EPOX}\cdot[EPOX] = 26.5\ \mu s^{-1}$. Next, as we do not work oxygen-free, the T_1 state of the ITX will be quenched by oxygen. The corresponding rate can be estimated by $\gamma_{ox} = 4\ \mu s^{-1}$.[45] Finally, there is the desired triplet quenching via electron transfer to the onium. In the case of Ar_3S^+, the molar quenching rate is found to be $k_{Ar_3S} = 210\ M^{-1}\ \mu s^{-1}$.[30] With a concentration of Ar_3S^+ units of $[Ar_3S^+] = 10.73$ mM, we end up with $\gamma_{Ar_3S} = 2.25\ \mu s^{-1}$. Without TAD, the total quenching rate is therefore $\gamma_{noTAD} = \gamma_0 + \gamma_{EPOX} + \gamma_{Ox} + \gamma_{Ar3S} = 32.8\ \mu s^{-1}$. The inverse of it, $\tau_T = 30$ ns, is actually the lifetime

https://doi.org/10.1021/acs.jpcc.3c04394
J. Phys. Chem. C 2023, 127, 18736−18744

of the ITX triplet state within the resist, and the quantum efficiency for an electron transfer is $\eta_{elT,\ noTAD} = \gamma_{Ar3S}/\gamma_{noTAD} = 6.9\%$. We also note in passing that working oxygen-free would increase this efficiency only to 7.8%, so it is not worth the effort to exclude the oxygen, as usual when working with cationic polymerization.

We now can turn to theoretically estimate P_{sat}, which we define as the TAD power, where the polymerization, which is initiated by electron transfer, is reduced down to $1/e$. This means that the quantum efficiency for an electron transfer with the depleting beam switched on needs to decrease down to $1/e$, or

$$\eta_{elT,TAD} = \frac{\eta_{elT,noTAD}}{e} \tag{2}$$

whereby $\eta_{elT,\ TAD} = \gamma_{Ar3S}/(\gamma_{noTAD} + \gamma_{TAD})$, which leads to the condition

$$\gamma_{TAD} = (e-1)\cdot\gamma_{noTAD} \tag{3}$$

From the above discussion about the branching ratio between RISC and IC from T_n back down to T_1, it follows that $\gamma_{TAD} = \gamma_{TT}\cdot\eta_{esc}$, whereby the triplet−triplet absorption rate γ_{TT} can be estimated from published oscillator strengths. Rai-Constapel et al. showed that, within the triplet system, the $T_1 \rightarrow T_8$ transition is by far the dominating one with an oscillator strength of $f = 0.33$,[35] in accordance with Harke et al., who calculated $f = 0.26$ for the $T_1 \rightarrow T_8$ transition.[26] Without specifying the final T_n state, Mundt et al. found $f = 0.28$.[36] We therefore assume that $f \approx 0.3$ is a reasonable average. From this, we can deduce (see the Supporting Information) an absorption cross section in the peak of the transient absorption spectrum of $\sigma_{TT,max} = 7.83 \times 10^{-17}$ cm^2. This peak is at about 630 nm, with a 60 nm full-width at half-maximum.[26] Therefore, we assume the triplet−triplet absorption cross section at 660 nm (the wavelength of the TAD laser) to be $\sigma_{TT} = 3.9 \times 10^{-17}$ cm^2.

The diffraction-limited diameter of the ordinarily shaped PSF of the TAD beam used for the depletion measurements is 220 nm, and therefore, the depletion area can be estimated by $A = 3.80 \times 10^{-10}$ cm^2. The photon flux density in the focus is given by

$$\Phi_{TAD} = \frac{P_{TAD}\cdot T\cdot\lambda}{A\cdot h\cdot c} \tag{4}$$

with P_{TAD} being the TAD power going into the objective lens, $T = 0.9$ being the transmission of the objective lens at $\lambda = 660$ nm (specified by the manufacturer), h being Planck's constant, and c is the speed of light. With the equality $\gamma_{TT} = \Phi_{TAD}\cdot\sigma_{TT}$ and eqs 3 and 4, we arrive at the following formula for the saturation power, where the polymerization should have dropped down to $1/e$ of its original value:

$$P_{sat} = \frac{hc}{\lambda}\cdot\frac{A}{\sigma_{TT}}\cdot\frac{e-1}{T\cdot\eta_{esc}}\gamma_{noTAD} \tag{5}$$

Inserting all numerical values, we receive $P_{sat} = 3.4$ mW. This is twice the experimental value of 1.7 mW (Figure 2a); however, it is remarkably close to it, considering how many parameters went into this estimation. We stress that all values were reasonably based upon published data (either experimental or theoretical) of the dynamics of ITX or closely related thioxanthones. The largest uncertainty probably lies in the rate of RISC. This was assumed to be similar to the rate of ISC, for which published data vary from $(10\ ps)^{-1}$ to $(4\ ps)^{-1}$.[31,33,35] Furthermore, it is reasonable to assume that due to Fermi's golden rule, the rate of RISC is larger than that of ISC because of the higher density of the final RISC states within the highly excited singlet system compared to the low number of triplet levels in the range of T_1 and T_2 available for ISC. This would increase the escape efficiency η_{esc} and consequently reduce the theoretically estimated value for P_{sat}. Finally, we would like to stress that our above considerations on the TAD process in ITX as a photosensitizer for cationic polymerization also shed light on the TAD process in the case of ITX as a one-component type II starter for radical polymerization.[40] Instead of an electron transfer to an onium, hydrogen abstraction within the same or from another ITX molecule takes place.[37] To the best of our knowledge, it has so far not been considered in detail why RISC can actually outperform the intratriplet IC back to the T_1 followed by hydrogen abstraction. In a similar way, the radical starters 7-diethylamino-3-thenoylcoumarin (DETC),[24] Michler's ethyl ketone,[43] or some diketones[47] are depletable by TAD, and a similar consideration as outlined above might be applied to explain the intramolecular dynamics that renders TAD effective in the case of radical polymerization lithography using these starters.

DISCUSSION

When comparing the depletion efficiencies of $Ar_3S{:}SbF_6$ and $Ph_2I{:}PF_6$, it appears that $Ar_3S{:}SbF_6$ is more effective than $Ph_2I{:}PF_6$. This is clearly seen when comparing the saturation powers in Figure 2, which are 1.7 ± 0.2 and 8.1 ± 1.6 mW in the case of $Ar_3S{:}SbF_6$ and $Ph_2I{:}PF_6$, respectively. This is almost a factor of 5 difference. However, this can be explained if one has a closer look at the electron transfer process. It is allowed if

$$\Delta G = E_{ox,ITX} - E_T - E_{red,on} \tag{6}$$

is negative.[46] Here, $E_{ox,ITX}$ is the ground-state oxidation potential of ITX, E_T is the triplet energy of ITX above the S_0, and $E_{red,on}$ is the reduction potential of the onium. While $\Delta G < 0$ holds for both Ar_3S^+ and Ph_2I^+, it is well-documented that the reduction potential of Ph_2I^+ is some 100 mV less negative than that of Ar_3S^+, and therefore, ΔG is more negative in the case of Ph_2I^+ compared to Ar_3S^+ as an electron acceptor.[30,46,48] This has the consequence that electron transfer from a triplet ITX to Ph_2I^+ is up to a factor of 10 more feasible than to Ar_3S^+.[30] This shortens the T_1 lifetime (or increases γ_{noTAD} and hence P_{sat} in eq 5). Consequently, more TAD power is needed so that RISC can compete with (and finally outperform) electron transfer. This theoretical consideration nicely fits to our experimental result that P_{sat} is larger in the case of $Ph_2I{:}PF_6$ compared to $Ar_3S{:}SbF_6$, see Figure 2.

Next, we give a plausible explanation for the undepletable residuum in the height of the lines in Figure 2 and, simultaneously, for the pedestal that appears when more than 1 mW of 660 nm light is applied and broadens upon a further increase of the 660 nm TAD power (Figure 3b, open circles). Obviously, this polymerization cannot be stopped by 660 nm and even grows in width with increasing 660 nm power. Hence, the initiation of polymerization should be of a different nature than the so far discussed route of electron transfer followed by the formation of an $ITX^{\cdot+}$ radical cation. Furthermore, the pedestal also appears when an ordinarily shaped (instead of a donut-shaped) PSF of 660 nm light is applied, see Supporting Information, Figure S3.

https://doi.org/10.1021/acs.jpcc.3c04394
J. Phys. Chem. C 2023, 127, 18736−18744

Indeed, there is an alternative possibility, which is shown in Figure 4 on the upper right. Starting from the T_1, the absorption of a 660 nm photon excites the ITX to a higher triplet state T_n, possibly the T_8. From there, it has sufficient energy that a triplet energy transfer from the ITX toward the onium can take place, leaving the onium in an excited triplet state, which promptly dissociates into an aryl-onium radical cation and an aryl cation.[21,45] This is the natural way how onium salts initiate cationic polymerizations if excited directly in the UV region. Most important, this polymerization path is inaccessible to further manipulation with light; hence, this is a dark reaction path, and TAD cannot be used for depletion. Further, as an energy transfer has a typical rate on the order of $\gamma_{ET} = (500\ \text{ps})^{-1}$, this process is rather sluggish compared to the electron transfer route and hence only appears at high powers of 660 nm light. Nevertheless, it competes with the photoinitiation via the electron transfer process. Hence, the faster the electron transfer is, the less effective is the triplet energy transfer route. Above, we noted that ΔG is more negative for Ph_2I^+ compared to Ar_3S^+, and hence, P_{sat} is smaller in the case of $Ar_3S{:}SbF_6$ compared to $Ph_2I{:}PF_6$. The same reason, the more negative ΔG, disfavors the triplet energy transfer route with respect to the optically depletable electron transfer route, and hence, the residuum is larger in the case of the $Ar_3S{:}SbF_6$ compared to $Ph_2I{:}PF_6$. Consequently, the smaller P_{sat} and the larger residuum in the exponential fit in the case of $Ar_3S{:}SbF_6$ (Figure 2a) as compared to $Ph_2I{:}PF_6$ (Figure 2b) can both be traced back to the more negative ΔG in the case of Ph_2I^+.

While the broad pedestals that start to appear at around 2 mW have now been associated to being caused by energy transfer, we assign the thin (and depletable) central lines to being started by electron transfer. This route can effectively be depleted by TAD. Hence, the linewidths narrow from 350 down to 130 nm when increasing the TAD power up to 1.5 mW. However, beyond this TAD power, they start to broaden again until they reach the original width of approx. 350 nm. This means that TAD becomes less effective with increasing power and eventually ceases to have any influence on the linewidth. We argue that local heating might be responsible for this effect. The 660 nm beam pumps quite some energy into the system.[49] First, it cycles the ITX molecule within the triplet system between T_1 and T_n, whereby the intratriplet IC releases thermal energy. If, eventually, RISC occurs, further thermal energy is liberated due to the IC within the singlet system. This local increase of thermal energy can have two consequences. First, the electron transfer from the triplet system to the onium is thermally activated via the T_2 state. Thus, increased thermal energy renders the electron transfer more efficient, and hence, TAD becomes less efficient in relation to the energy transfer. The second reason might be that a local heating yields a local decrease in viscosity, and therefore, the $ITX^{\cdot+}$ and the initially activated monomers become more mobile, which increases the area, where polymerization can occur.[50] The latter effect might also contribute to the increasing widening of the pedestal with increasing 660 nm power. However, we note that the line height as a function of TAD power seems to converge to a constant residuum and does not increase again, at least not in the investigated power range, which was technically limited by the onset of microexplosions. Further research is needed to clarify this.

CONCLUSIONS

We have shown, for the first time, that STED-inspired photoinhibition lithography can be achieved with cationic photoinitiated epoxides. This is achieved by using ITX and a sulfonium salt as the photoinitiating species. After two-photon excitation, ITX can be depleted via transient-state absorption (TAD), and the electron transfer from the triplet ITX to the sulfonium can be prevented. This way, no $ITX^{\cdot+}$ radical cations form and polymerization is suppressed in the outer rim of the excitation point spread function when a 660 nm TAD laser is applied in a donut shape around the central two-photon excitation focus. Linewidths of 130 nm could be achieved, which are only one-third of the linewidths achievable with pure two-photon lithography. Different from acrylate-based STED-inspired photoinhibition lithography, the polymerization could not be suppressed completely. We attribute this to the fact that the ITX, excited to a high triplet level by the 660 nm TAD beam, can sensitize the sulfonium via triplet energy transfer. Subsequently, the sulfonium dissociates and initiates epoxide polymerization, which we assign for being responsible for the undepletable pedestal underneath the thin depletable lines. Further, the repeated intratriplet internal conversion and the intrasinglet IC both dump thermal energy into the focal area, which increases the mobility of the starters and hence might contribute to the observed broadening of both the pedestal and the central line. Further, the additional thermal energy may lead to an accelerated electron transfer and therefore renders TAD less efficient.

This picture conclusively describes most of our experimental findings, although we admit that further research is necessary to complete the picture. However, this work represents, to the best of our knowledge, the first STED-inspired photopolymerization lithography beyond radically polymerizing resins. We addressed several critical points to render TAD efficient, such as the branching ratio of reverse intersystem crossing and intratriplet internal conversion, or the quantum efficiency of TAD, competing with a thermally activated electron transfer, triplet quenching by the monomers and, in the case of higher TAD powers, with triplet energy transfer. Future work has to optimize these branching ratios in order to make TAD more efficient and to increase the writing speed. Currently, we are only able to write supported lines, while experiments trying to write higher dimensional structures such as suspended lines, or lower-dimensional structures such as individual voxels, failed so far. Also, postbaking steps could not improve the outcome of our experiments with EPOX. We are, however, very optimistic that three-dimensional nanoscale structures will be realized in the near future, possibly with other epoxide monomers that allow for better cross-linking and pre- and postbaking or postexposure routines. We are confident that our experimental findings and theoretical considerations substantially help to guide the way toward efficient STED-inspired subdiffractional lithography using cationic polymerization.

ASSOCIATED CONTENT

Supporting Information

The Supporting Information is available free of charge at https://pubs.acs.org/doi/10.1021/acs.jpcc.3c04394.

TAD efficiencies for various ITX and onium concentrations, development of the pedestal as a function of TAD power using an ordinary 660 nm PSF, SEM images

https://doi.org/10.1021/acs.jpcc.3c04394
J. Phys. Chem. C 2023, 127, 18736−18744

of four runs of photoinhibition experiments and evaluation of linewidths, TAD photoinhibition lines with $Ph_2I:PF_6$ as the initiator, and calculation of σ_{TT} from oscillator strength f (PDF)

AUTHOR INFORMATION

Corresponding Author

Thomas A. Klar − *Institute of Applied Physics, Johannes Kepler University Linz, 4040 Linz, Austria;* orcid.org/0000-0002-1339-5844; Email: thomas.klar@jku.at

Authors

Sourav Islam − *Institute of Applied Physics, Johannes Kepler University Linz, 4040 Linz, Austria*

Marco Sangermano − *Department of Applied Science and Technology, Politecnico Di Torino, 10124 Torino, Italy;* orcid.org/0000-0002-8630-1802

Complete contact information is available at: https://pubs.acs.org/10.1021/acs.jpcc.3c04394

Funding

Open Access is funded by the Austrian Science Fund (FWF).

Notes

The authors declare no competing financial interest.

ACKNOWLEDGMENTS

We thank Heidi Piglmayer-Brezina for lab assistance, specifically for taking the SEM images, Bernhard Fragner and Alfred Nimmervoll for technical assistance, and Lorenzo Pezzana for discussions and assistance in chemical experiments. This work was funded by the Austrian Science Fund (FWF) via the Doctorate College program "Nano-Analytics of Cellular Systems" (NanoCell, grant number W 1250) and via the project P 31827.

REFERENCES

(1) Strickler, J. H.; Webb, W. W. Three-dimensional optical data storage in refractive media by two-photon point excitation. *Opt. Lett.* **1991**, *16*, 1780−1782.

(2) Kawata, S.; Sun, H. B.; Tanaka, T.; Takada, K. Finer features for functional microdevices. *Nature* **2001**, *412*, 697−698.

(3) Fischer, J.; Wegener, M. Three-dimensional optical laser lithography beyond the diffraction limit. *Las. Phot. Rev.* **2013**, *7*, 22−44.

(4) Hell, S. W.; Wichmann, J. Breaking the diffraction resolution limit by stimulated emission: stimulated-emission-depletion fluorescence microscopy. *Opt. Lett.* **1994**, *19*, 780−782.

(5) Klar, T. A.; Hell, S. W. Subdiffraction resolution in far-field fluorescence microscopy. *Opt. Lett.* **1999**, *24*, 954−956.

(6) Hofmann, M.; Eggeling, C.; Jakobs, S.; Hell, S. W. Breaking the diffraction barrier in fluorescence microscopy at low light intensities by using reversibly photoswitchable proteins. *Proc. Natl. Acad. Sci. U. S. A.* **2005**, *102*, 17565−17569.

(7) Scott, T. F.; Kowalski, B. A.; Sullivan, A. C.; Bowman, C. N.; McLeod, R. R. Two-Color Single-Photon Photoinitiation and Photoinhibition for Subdiffraction Photolithography. *Science* **2009**, *324*, 913−917.

(8) Li, L.; Gattass, R. R.; Gershgoren, E.; Hwang, H.; Fourkas, J. T. Achieving $\lambda/20$ Resolution by One-Color Initiation and Deactivation of Polymerization. *Science* **2009**, *324*, 910−913.

(9) Fischer, J.; von Freymann, G.; Wegener, M. The Materials Challenge in Diffraction-Unlimited Direct-Laser-Writing Optical Lithography. *Adv. Mater.* **2010**, *22*, 3578−3582.

(10) Cao, Y. Y.; Gan, Z.; Jia, B.; Evans, R. A.; Gu, M. High-photosensitive resin for super-resolution direct-laser-writing based on photoinhibited polymerization. *Opt. Exp.* **2011**, *19*, 19486−19494.

(11) Wollhofen, R.; Katzmann, J.; Hrelescu, C.; Jacak, J.; Klar, T. A. 120 nm resolution and 55 nm structure size in STED-lithography. *Opt. Exp.* **2013**, *21*, 10831−10840.

(12) He, M.; Zhang, Z.; Cao, C.; Zhou, G.; Kuang, C.; Liu, X. 3D Sub-Diffraction Printing by Multicolor Photoinhibition Lithography: From Optics to Chemistry. *Laser Photonics Rev.* **2022**, 2100229.

(13) Mueller, P.; Zieger, M. M.; Richter, B.; Quick, A. S.; Fischer, J.; Mueller, J. B.; Zhou, L.; Nienhaus, G. U.; Bastmeyer, M.; Barner-Kowollik, C.; et al. Molecular Switch for Sub-Diffraction Laser Lithography by Photoenol Intermediate-State Cis-Trans Isomerization. *ACS Nano* **2017**, *11*, 6396−6403.

(14) Vijayamohanan, H.; Kenath, G. S.; Palermo, E. F.; Ullal, C. K. Super-resolution interference lithography enabled by non-equilibrium kinetics of photochromic monolayers. *RSC Adv.* **2019**, *9*, 28841−28850.

(15) Murtezi, E.; Puthukodan, S.; Buchegger, B.; Jacak, J.; Klar, T. A. STED controlled photobleaching for sub-diffractional optical nanopatterning. *J. Phys. Photonics* **2020**, *2*, No. 044003.

(16) Vijayamohanan, H.; Palermo, E. F.; Ullal, C. K. Spirothiopyran-Based Reversible Saturable Photoresist. *Chem. Mater.* **2017**, *29*, 4754−4760.

(17) Müller, P.; Müller, R.; Hammer, L.; Barner-Kowollik, C.; Wegener, M.; Blasco, E. STED-Inspired Laser Lithography Based on Photoswitchable Spirothiopyran Moieties. *Chem. Mater.* **2019**, *31*, 1966−1972.

(18) Sangermano, M. Advances in cationic photopolymerization. *Pure Appl. Chem.* **2012**, *84*, 2089−2101.

(19) Boiko, Y.; Costa, J. M.; Wang, M.; Esener, S. Cationic two-photon induced polymerisation with high dynamic range. *Opt. Exp.* **2001**, *8*, 571−584.

(20) Tottori, S.; Zhang, L.; Qiu, F.; Krawczky, K. K.; Franco-Obregon, A.; Nelson, B. J. Magnetic Helical Micromachines: Fabrication, Controlled Swimming, and Cargo Transport. *Adv. Mater.* **2012**, *24*, 811−816.

(21) Crivello, J. V.; Lam, J. H. W. Diaryliodonium Salts. A New Class of Photoinitiators for Cationic Polymerization. *Macromolecules* **1977**, *10*, 1307−1315.

(22) Crivello, J. V.; Lam, J. H. W. Photoinitiated cationic polymerization with triarylsulfonium salts. *J. Polym. Sci., Part A: Polym. Chem.* **1979**, *17*, 977−999.

(23) Crivello, J. V.; Lam, J. H. W. Dye-sensitized photoinitiated cationic polymerization. *J. Polym. Sci., Polym. Chem. Ed.* **1978**, *16*, 2441−2451.

(24) Wolf, T. J. A.; Fischer, J.; Wegener, M.; Unterreiner, A. N. Pump-probe spectroscopy on photoinitiators for stimulated-emission-depletion optical lithography. *Opt. Lett.* **2011**, *36*, 3188−3190.

(25) Harke, B.; Bianchini, P.; Brandi, F.; Diaspro, A. Photopolymerization Inhibition Dynamics for Sub-Diffraction Direct Laser Writing Lithography. *ChemPhysChem* **2012**, *13*, 1429−1434.

(26) Harke, B.; Dallari, W.; Grancini, G.; Fazzi, D.; Brandi, F.; Petrozza, A.; Diaspro, A. Polymerization Inhibition by Triplet State Absorption for Nanoscale Lithography. *Adv. Mater.* **2013**, *25*, 904−909.

(27) Chi, T.; Somers, P.; Wilcox, D. A.; Schuman, A. J.; Iyer, V.; Le, R.; Gengler, J.; Ferdinandus, M.; Liebig, C.; Pan, L.; et al. Tailored Thioxanthone-Based Photoinitiators for Two-Photon-Controllable Polymerization and Nanolithographic Printing. *J. Polym. Sci., Part B: Polym. Phys.* **2019**, *57*, 1462−1475.

(28) Chi, T.; Somers, P.; Wilcox, D. A.; Schuman, A. J.; Johnson, J. E.; Lisang, Z.; Pan, L.; Xu, X.; Boudouris, B. W. Substituted Thioxanthone-Based Photoinitiators for Efficient Two-Photon Direct Laser Writing Polymerization with Two-Color Resolution. *ACS Appl. Polym. Mater.* **2021**, *3*, 1426−1435.

(29) Amirzadeh, G.; Schnabel, W. On the Photoinitiation of Free Radical Polymerization Laser Flash Photolysis Investigations on Thioxanthone Derivatives. *Makromol. Chem.* **1981**, *182*, 2821−2835.

(30) Kunze, A.; Müller, U.; Tittes, K.; Fouassier, J. P.; Morlet-Savary, F. Triplet quenching by onium salts in polar and nonpolar solvents. *J. Photochem. Photobiol., A* **1997**, *110*, 115−122.
(31) Cook, W. D.; Chen, S.; Chen, F.; Kahveci, M. U.; Yagci, Y. Photopolymerization of Vinyl Ether Networks Using an Iodonium Initiator—The Role of Photosensitizers. *J. Polym. Sci., Part A: Polym. Chem.* **2009**, *47*, 5474−5487.
(32) Angulo, G.; Grilj, J.; Vauthey, E.; Serrano-Andrés, L.; Rubio-Pons, Ò.; Jacques, P. Ultrafast Decay of the Excited Singlet States of Thioxanthone by Internal Conversion and Intersystem Crossing. *ChemPhysChem* **2010**, *11*, 480−488.
(33) Rai-Constapel, V.; Salzmann, S.; Marian, C. M. Isolated and Solvated Thioxanthone: A Photophysical Study. *J. Phys. Chem. A* **2011**, *115*, 8589−8596.
(34) Villnow, T.; Rysek, G.; Rai-Constapel, V.; Marian, C. M.; Gilch, P. Chimeric Behavior of Excited Thioxanthone in Protic Solvents: I. Experiments. *J. Phys. Chem. A* **2014**, *118*, 11696−11707.
(35) Rai-Constapel, V.; Villnow, T.; Rysek, G.; Gilch, P.; Marian, C. M. Chimeric Behavior of Excited Thioxanthone in Protic Solvents: II. Theory. *J. Phys. Chem. A* **2014**, *118*, 11708−11717.
(36) Mundt, R.; Villnow, T.; Torres Ziegenbein, C.; Gilch, P.; Marian, C. M.; Rai-Constapel, V. Thioxanthone in apolar solvents: ultrafast internal conversion precedes fast intersystem crossing. *Phys. Chem. Chem. Phys.* **2016**, *18*, 6637−6647.
(37) Dadashi-Silab, S.; Aydogan, C.; Yagci, Y. Shining a light on an adaptable photoinitiator: advances in photopolymerizations initiated by thioxanthones. *Polym. Chem.* **2015**, *6*, 6595−6615.
(38) Mau, A.; Le, T. H.; Dietlin, C.; Bui, T.-T.; Graff, B.; Dumur, F.; Goubard, F.; Lalevee, J. Donor-acceptor-donor structured thioxanthone derivatives as visible photoinitiators. *Polym. Chem.* **2020**, *11*, 7221−7234.
(39) Johnson, J. E.; Chen, Y.; Xu, X. Model for polymerization and self-deactivation in two-photon nanolithography. *Opt. Exp.* **2022**, *30*, 26824−26840.
(40) Liaros, N.; Gutierrez-Razo, S. A.; Thum, M. D.; Ogden, H. M.; Zeppuhar, A. N.; Wolf, S.; Baldacchini, T.; Kelley, M. J.; Petersen, J. S.; Falvey, D. E.; et al. Elucidating complex triplet-state dynamics in the model system isopropylthioxanthone. *iScience* **2022**, *25*, No. 103600.
(41) Kunik, D.; Luduena, S. J.; Costantino, S.; Martinez, O. E. Fluorescent two-photon nanolithography. *J. Microsc.* **2008**, *229*, 540−544.
(42) Westphal, V.; Hell, S. W. Nanoscale resolution in the focal plane of an optical microscope. *Phys. Rev. Lett.* **2005**, *94*, No. 143903.
(43) Gvindzhiliia, G.; Sivun, D.; Naderer, C.; Jacak, J.; Klar, T. A. Low-Fluorescence Starter for Optical 3D Lithography of Sub-40 nm Structures. *ACS Applied Opt. Mater.* **2023**, *1*, 945−951.
(44) El-Sayed, M. A. Spin-Orbit Coupling and the Radiationless Processes in Nitrogen Heterocyclics. *J. Chem. Phys.* **1963**, *38*, 2834−2838.
(45) Manivannan, G.; Fouassier, J. P. Primary Process in the Photosensitized Polymerization of Cationic Monomers. *J. Polym. Sci., Part A: Polym. Chem.* **1991**, *29*, 1113−1124.
(46) Sundell, P. E.; Jönsson, S.; Hult, A. Photo-Redox Induced Cationic Polymerization of Divinyl Ethers. *J. Polym. Sci., Part A: Polym. Chem.* **1991**, *29*, 1525−1533.
(47) Bojanowski, N. M.; Vranic, A.; Hahn, V.; Rietz, P.; Messer, T.; Brückel, J.; Barner-Kowollik, C.; Blasco, E.; Bräse, S.; Wegener, M. Search for Alternative Two-Step-Absorption Photoinitiators for 3D Laser Nanoprinting. *Adv. Funct. Mater.* **2022**, 2212482.
(48) Hola, E.; Pilch, M.; Ortyl, J. Thioxanthone Derivatives as a New Class of Organic Photocatalysts for Photopolymerisation Processes and the 3D Printing of Photocurable Resins under Visible Light. *Catalysts* **2020**, *10*, 903.
(49) Allonas, X.; Ley, C.; Bibaut, C.; Jacques, P.; Fouassier, J. P. Investigation of the triplet quantum yield of thioxanthone by time-resolved thermal lens spectroscopy: solvent and population lens effects. *Chem. Phys. Lett.* **2000**, *322*, 483−490.
(50) Takada, K.; Kaneko, S.; Li, Y.-D.; Kawata, S.; Chen, Q.-D.; Sun, H.-B. Temperature effects on pinpoint photopolymerization and polymerized micronanostructures. *Appl. Phys. Lett.* **2008**, *92*, No. 041902.

https://doi.org/10.1021/acs.jpcc.3c04394
J. Phys. Chem. C 2023, 127, 18736−18744